Large-cutoff behavior of local chiral effective field theory interactions

I. Tews,[1,2,*] L. Huth,[3,4,†] and A. Schwenk[3,4,5,‡]

[1]*Institute for Nuclear Theory, University of Washington, Seattle, Washington 98195-1550, USA*

[2]*JINA-CEE, Michigan State University, East Lansing, Michigan, 48823, USA*

[3]*Institut für Kernphysik, Technische Universität Darmstadt, 64289 Darmstadt, Germany*

[4]*ExtreMe Matter Institute EMMI, GSI Helmholtzzentrum für Schwerionenforschung GmbH, 64291 Darmstadt, Germany*

[5]*Max-Planck-Institut für Kernphysik, Saupfercheckweg 1, 69117 Heidelberg, Germany*

(Received 19 June 2018; published 22 August 2018)

Interactions from chiral effective field theory have been successfully employed in a broad range of *ab initio* calculations of nuclei and nuclear matter, but it has been observed that most results of few- and many-body calculations experience a substantial residual regulator and cutoff dependence. In this work, we investigate the behavior of local chiral potentials at leading order under variation of the cutoff scale for different local regulators. When varying the cutoff, we require that the resulting interaction produces no spurious bound states in the deuteron channel. We find that, for a particular choice of leading-order operators, nucleon-nucleon phase shifts and the deuteron ground-state energy converge to cutoff-independent plateaus for all regulator functions we investigate. This observation may enable improved calculations with chiral Hamiltonians that also include three-nucleon interactions.

DOI: 10.1103/PhysRevC.98.024001

I. INTRODUCTION

Chiral effective field theory (EFT) [1,2] has been shown to be a powerful framework to derive nuclear interactions. It provides a systematic expansion for nuclear forces that is linked to the symmetries of quantum chromodynamics (QCD). This systematic expansion is based on a so-called power-counting (PC) scheme that ideally allows one to arrange different contributions to the interaction according to their importance. Thus, the PC scheme establishes a truncation scheme, which enables one to obtain systematic uncertainty estimates.

Modern chiral EFT interactions are typically constructed by applying Weinberg power counting (WPC) [3–6], which is based on dimensional analysis in momentum space. In the purely pionic and one-nucleon sector, due to the Goldstone-boson nature of pions, all amplitudes can be expanded in powers of the dimensionless expansion parameter Q/Λ_b, where Q is a typical momentum of the system and Λ_b is the breakdown scale of the theory. In the two-nucleon sector, instead, bound states appear and the problem becomes nonperturbative. To obtain observables, WPC suggests defining the nuclear potential as the sum of all irreducible diagrams that do not contain purely nucleonic intermediate states and thus are not infrared enhanced. This sum is then truncated according to a power counting in Q/Λ_b. The resulting potential is iterated to all orders by solving the Lippmann-Schwinger (LS) or Schrödinger equation. At the two-body level, at leading order (LO), WPC leads to the appearance of S-wave contact interactions and the one-pion-exchange (OPE) interaction, while at higher orders additional derivative contact interactions and multipion-exchange interactions, as well as corrections to previous topologies, have to be considered.

This approach has unsolved problems. In few- and many-body calculations, a regularization scheme has to be introduced to cut off high-momentum modes that may lead to divergences. Because the regularization scheme is arbitrary, results should be independent of this choice after the dependence of contact parameters on the regularization scale, the so-called cutoff Λ_c, is taken into account. This means that at each order there should be sufficiently many counterterms to absorb any residual cutoff dependence in the limit $\Lambda_c \to \infty$. This is problematic for singular potentials, such as OPE, which has a $1/r^3$ behavior in spin $S = 1$ channels due to the tensor force. Although the focus is to describe long-range behavior, this singular potential nevertheless generates an oscillatory wave function for $r \to 0$ that leads to the appearance of spurious bound states and cutoff-dependent results. To renormalize such a potential in a certain partial wave, i.e., to obtain cutoff-independent results for large cutoffs, a counterterm is necessary in the same partial wave [7,8]. In WPC at LO, however, the only counterterms appear in the S waves but not in partial waves with orbital angular momentum $l > 0$, where the singular OPE potential also contributes.

Kaplan, Savage, and Wise (KSW) [9,10] suggested a different PC that uses dimensional regularization (DR) with power divergence subtraction to systematically expand the nucleon-nucleon (NN) scattering amplitude in powers of Q/Λ_b instead of the potential. Within this scheme, only the LO contact interactions are treated nonperturbatively, while other contact interactions and pion exchanges are treated in

*itews@uw.edu

†lukashuth@theorie.ikp.physik.tu-darmstadt.de

‡schwenk@physik.tu-darmstadt.de

finite order in perturbation theory, in order to find analytic expressions for the scattering amplitudes. Although the KSW power counting is well defined and consistent, it failed to reproduce the phase shifts from the Nijmegen partial-wave analysis (PWA) [11] in spin-triplet channels at next-to-next-to-leading order (N^{2}LO) [12] and led to large N^{2}LO corrections. It was found that in some spin-triplet channels, the nonperturbative treatment of pion-exchange diagrams is necessary at higher momenta because the OPE tensor force is large and singular and must be summed to all orders. This is done in WPC and reflects the fact that a correct renormalization of singular potentials is intrinsically nonperturbative [13]. A solution to this problem was suggested in Ref. [14], where the short-range part of the OPE interaction was canceled by fictitious heavy mesons.

Nogga, Timmermans, and van Kolck (NTvK) [8] studied the cutoff dependence of phase shifts at LO in WPC for nonlocal regulators and for a cutoff range of $\Lambda_c = 2$–20 fm^{-1}. They found that WPC leads to cutoff-independent results in the spin $S = 0$ channels, in the $^3S_1$ channel, where WPC includes a counterterm, and in $S = 1$ channels with repulsive tensor forces, e.g., $^3P_1$. However, NTvK observed strong cutoff dependences and the appearance of several spurious bound states in the other attractive tensor channels, $^3P_0$, $^3D_2$, and $^3P_2$-$^3F_2$, where there are no counterterms present in WPC. As a solution, NTvK suggested to explicitly add counterterms to partial waves with attractive tensor interactions, i.e., $^3P_0$, $^3P_2$, and $^3D_2$ (see also, e.g., Refs. [15,16]). In higher partial waves, NTvK found that the centrifugal barrier screened the singular tensor force sufficiently so that no counterterms were necessary in the investigated cutoff range. The modification of WPC proposed by NTvK was confirmed based on a renormalization group analysis [17], but also triggered a debate on whether it remains necessary in higher order descriptions of NN scattering; see, e.g., Ref. [18].

In this paper, we investigate the large-cutoff behavior of local chiral interactions that were introduced in Refs. [19,20]. It has been found that local regulators induce regulator artifacts, which mix contact interactions in a certain partial wave into all higher partial waves [21–23], because the regulator does not commute with the antisymmetrizer. These regulator artifacts have been analyzed in detail in Ref. [23] for chiral NN interactions at LO. In this work, we exploit these regulator artifacts to mix LO contact interaction terms into all attractive tensor channels to obtain cutoff-independent results for the phase shifts and deuteron ground-state energy.

This paper is organized as follows. In Sec. II, we introduce the local chiral interactions at LO that we consider in this work. In Sec. III, we then present the results for the phase shifts and the deuteron ground-state energy for these interactions and discuss the results in Sec. IV. Finally, we summarize in Sec. V.

II. LOCAL CHIRAL INTERACTIONS AT LO

At LO, local chiral potentials in coordinate space are given by

$$V_{\rm NN}^{\rm LO}(r, R_0) = V_{\rm OPE}^{\rm LO}(r, R_0) + V_{\rm cont}^{\rm LO}(r, R_0)\,, \tag{1}$$

with the OPE interaction

$$V_{\rm OPE}^{\rm LO}(r, R_0) = \frac{M_\pi^3}{12\pi}\left(\frac{g_A}{2F_\pi}\right)^2 \frac{e^{-M_\pi r}}{M_\pi r}\left\{\sigma_{12} + \left[1 + \frac{3}{M_\pi r} + \frac{3}{(M_\pi r)^2}\right] S_{12}\right\} \tau_{12}\, f_l(r, R_0)\,, \tag{2}$$

and the general set of contact interactions at LO, given by

$$V_{\rm cont}^{\rm LO}(r, R_0) = (C_1 + C_\sigma\,\sigma_{12} + C_\tau\,\tau_{12} + C_{\sigma\tau}\,\sigma_{12}\,\tau_{12})\, f_{\rm s}(r, R_0)\,, \tag{3}$$

where $\sigma_{12} = \boldsymbol{\sigma}_1 \cdot \boldsymbol{\sigma}_2$ and similar for τ_{12}. The contact interactions are generally fit to S-wave NN scattering. We use the long-range and short-range local regulator functions f_l and f_s,

$$f_l(r, R_0) = \left\{1 - \exp\left[-\left(\frac{r}{R_0}\right)^{n_1}\right]\right\}^{n_2}, \tag{4}$$

$$f_{\rm s}(r, R_0) = \frac{n}{4\pi\,\Gamma(3/n)\,R_0^3} \exp\left[-\left(\frac{r}{R_0}\right)^{n}\right], \tag{5}$$

with the coordinate-space cutoff R_0, and where n_1, n_2, and n determine the width of the regulator functions. In this work, we will investigate different combinations of n_1, n_2, and n for these regulator functions, as low-energy physics should be independent of the short-range details and any regulator function should be equally valid [7].

When the regulator commutes with the antisymmetrizer, as is the case for typical nonlocal regulators, only two of the four operators in Eq. (3) are linearly independent, and one can choose any two of the four operator structures for the LO potential (except $\mathbb{1}, \sigma_{12}\tau_{12}$ which is linearly dependent in the two S-wave channels). This is known as the Fierz ambiguity. From the spin-isospin LECs C_{ST}, which enter partial waves with spin S and the isospin T, one can then determine the operator LECs for different operator pairs according to

$$\begin{pmatrix} C_{00} \\ C_{01} \\ C_{10} \\ C_{11} \end{pmatrix} = \begin{pmatrix} 1 & -3 & -3 & 9 \\ 1 & -3 & 1 & -3 \\ 1 & 1 & -3 & -3 \\ 1 & 1 & 1 & 1 \end{pmatrix} \begin{pmatrix} C_{\mathbb{1}} \\ C_\sigma \\ C_\tau \\ C_{\sigma\tau} \end{pmatrix}. \tag{6}$$

However, the Fierz ambiguity is violated when local regulators are chosen; see Ref. [23] for a detailed discussion. In this case, when choosing two out of the four operators, the regulator affects the partial-wave decomposition and regulator artifacts appear in all higher partial waves. These artifacts have the form of higher order contact operators and their LECs depend on the LO operator choice. While this mixing of LO S-wave physics into higher partial waves cannot be turned off completely, one can construct interactions that vanish in the $ST = 00$ and $ST = 11$ partial waves, by choosing all four operators at LO and requiring $C_{00} = C_{11} = 0$. We denote the latter interaction LO$_{\rm n}P$, and it is closest to nonlocally regularized interactions.

In this work, we construct various potentials for different operator structures, different sets $\{n_1, n_2, n\}$, and different cutoff values in the range $R_0^{-1} = 0.8$–10.0 fm^{-1} in steps of 0.2 fm^{-1}, where we use the inverse of the coordinate-space cutoff because it is connected to the momentum-space cutoff. Then, large values for R_0^{-1} imply large momentum cutoffs. For each potential, we fit the two spin-isospin LECs in the

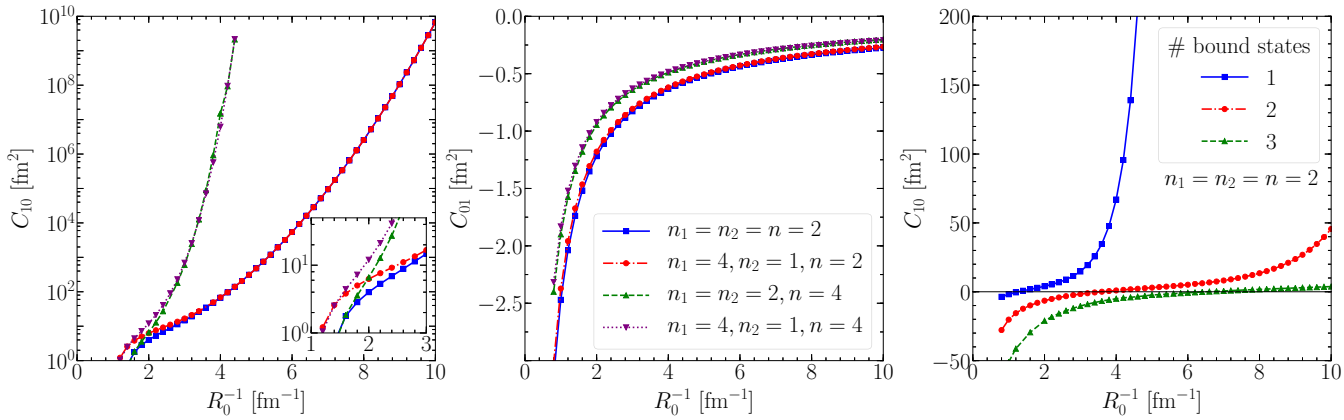

FIG. 1. Spin-isospin LECs C_{10} (left panel, logarithmic scale) and C_{01} (middle panel) as functions of the inverse cutoff R_0^{-1} for local chiral interactions at LO with different local regulators characterized by n_1, n_2, n. Right panel: Spin-isospin LEC C_{10} as function of the inverse cutoff R_0^{-1} for local chiral interactions at LO allowing one, two, and three bound states in the coupled ${}^3S_1$-${}^3D_1$ channel.

${}^1S_0$ and ${}^3S_1$ partial waves, C_{01} and C_{10}, to the corresponding S-wave phase shifts from the Nijmegen partial-wave analysis (PWA) [11] up to laboratory energies of 50 MeV, as in Ref. [23]. When varying R_0, we renormalize the LECs $C_{ST} = C_{ST}(R_0)$ to keep the phase shifts invariant at low energies. Depending on the size and sign of the LECs, we can obtain fits with an arbitrary number of bound states. Therefore, when fitting the LECs, we additionally require that the resulting interaction allows for exactly one bound state in the deuteron channel.

We present the resulting LECs C_{10} and C_{01} as functions of the inverse cutoff R_0^{-1} in the first two panels of Fig. 1, respectively, for four different sets $\{n_1, n_2, n\} = \{2, 2, 2\}$, $\{4, 1, 2\}$, $\{2, 2, 4\}$, and $\{4, 1, 4\}$. We find that the LEC dependence on the cutoff is regulator dependent, see also Ref. [8], and observe a systematic behavior for the different regulator choices in both ST channels.

We observe a strong increase of C_{10} with R_0^{-1} (in the left panel of Fig. 1), which is more prominent for short-range regulators with $n = 4$ (green and purple lines) compared to those with $n = 2$ (blue and red lines). This increase is due to the increasing attractive OPE tensor contribution in the $ST = 10$ channel when increasing R_0^{-1}. Because we only allow for one bound state in the deuteron channel, an increasing LEC is needed to balance the OPE attraction sufficiently so that no second bound state enters. We will discuss this in more detail later in this paper. For the interactions with $n = 4$, this requires a larger LEC because the regulator is sharper. Also, for $n = 4$ we could not achieve a fit beyond $R_0^{-1} = 4.4\,\mathrm{fm}^{-1}$, due to large numerical values and cancellations.

In the $ST = 10$ channel, at small values of R_0^{-1}, we find pairwise similar LECs for the sets $\{2, 2, 2\}$ (blue line) and $\{2, 2, 4\}$ (green line) as well as for the sets $\{4, 1, 2\}$ (red line) and $\{4, 1, 4\}$ (purple line). At large values of R_0^{-1} this behavior changes, and we find pairwise similar LECs for the sets $\{2, 2, 2\}$ (blue line) and $\{4, 1, 2\}$ (red line), and for the sets $\{2, 2, 4\}$ (green line) and $\{4, 1, 4\}$ (purple line). From this, we can deduce that at small R_0^{-1}, the LEC C_{10} is dominated by effects of the long-range regulator, while at large R_0^{-1}, the LEC is dominated by effects of the short-range regulator. The transition between those two regimes is found at cutoffs $R_0^{-1} \approx 2\,\mathrm{fm}^{-1}$. This transition region is shown in the inset in the left panel of Fig. 1. At small R_0^{-1}, the OPE is cut off at larger distances, and the LECs are rather small, so that the relative importance of the OPE is larger and the fits are mostly sensitive to the form of the long-range regulator. This changes at large R_0^{-1}, where differences in the long-range regulator are not so important because the short-range interactions cut off the OPE at a certain distance scale, independent of the long-range regulator function.

In the second panel of Fig. 1 we show the LEC C_{01}. We again observe pairwise similar LECs for the sets $\{2, 2, 2\}$ (blue line) and $\{4, 1, 2\}$ (red line) and for the sets $\{2, 2, 4\}$ (green line) and $\{4, 1, 4\}$ (purple line), but this time we observe no crossing with R_0^{-1}. The LEC C_{01} is mostly affected by the choice of the short-range regulator because the singular tensor force does not contribute to the ${}^1S_0$ channel and the OPE is relatively weak. This is reflected in the LECs, which are attractive, but approach zero for increasing R_0^{-1}. The LECs can be described with high precision by a function of the form

$$C_{01}(R_0) = a R_0^b \,. \tag{7}$$

For the sets $\{2, 2, 2\}$ and $\{4, 1, 2\}$ with $n = 2$, we find $a = -2.47\,\mathrm{fm}^{2+b}$ and $b = -0.98$. For the sets $\{2, 2, 4\}$ and $\{4, 1, 4\}$ with $n = 4$, we find $a = -1.83\,\mathrm{fm}^{2+b}$ and $b = -0.96$. Thus, the LECs are proportional to R_0^{-1}.

In the third panel, we show the LEC C_{10} when enforcing different numbers (one, two, or three) of bound states in the deuteron channel. As before, we observe a systematic behavior of the LECs with increasing R_0^{-1} but the LECs increase much slower for interactions with more bound states. We note that if we allow more bound states in the deuteron channel, this also leads to spurious bound states in higher partial waves with spin $S = 1$.

In Fig. 2, we show the potentials in the ${}^3S_1$ partial wave, as well as the corresponding wave functions, for one allowed

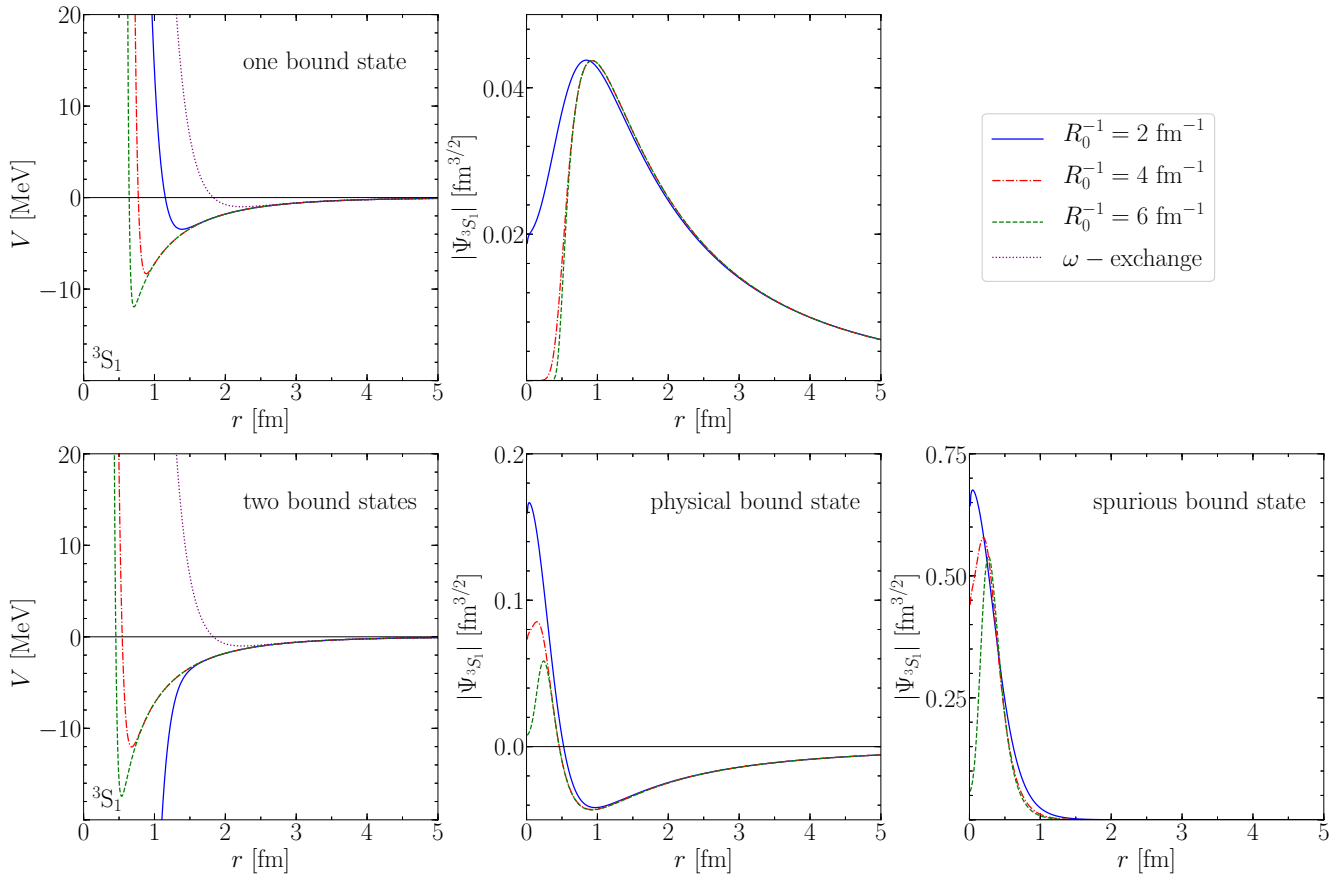

FIG. 2. Chiral LO potentials in the $^3S_1$ partial wave as well as the corresponding wave functions for one or two bound states for three cutoff values and $n_1 = n_2 = n = 2$. In addition, we compare the chiral LO potentials with a potential where the short-range interaction is replaced by an ω-meson-exchange potential.

bound state (upper panels) and when enforcing two bound states (lower panels) for three cutoff values. In the former case, for increasing R_0^{-1}, the OPE extends to smaller distances, but is cut off at small r by the repulsive short-range contact interaction. When increasing R_0^{-1} the range of the short-range regulator function decreases as expected, but this is compensated by very large LECs. This results in a hard core which does not vanish even for large values of R_0^{-1}, but cuts off the long-distance singular OPE in such a way that only one bound state can be accommodated.

These considerations allow us to understand the large-cutoff behavior of C_{10} in Fig. 1. To cut off the OPE at a certain radius scale $r^{*,i}$ so that only i bound states appear requires the short-range part of the potential at this scale to be sufficiently repulsive. For $n = 2$, we have

$$V_{10}(r^{*,i}) = C_{10}\frac{1}{\pi^{\frac{3}{2}}R_0^3}\exp\left[-\left(r^{*,i}R_0^{-1}\right)^2\right] = V_0^i\,, \qquad (8)$$

where V_{10} is the potential in the $^3S_1$ channel and V_0^i is the strength necessary to compensate the OPE at $r^{*,i}$. Then, it is easy to see that

$$C_{10} = V_0^i\pi^{\frac{3}{2}}R_0^3\exp\left[\left(r^{*,i}R_0^{-1}\right)^2\right], \qquad (9)$$

so C_{10} has to grow exponentially in R_0^{-2}, which is what we observe in Fig. 1. In fact, fitting the large-cutoff behavior for C_{10} in the case of one bound state, we find $C_{10} \sim \exp\left[(r^{*,1}R_0^{-1})^b\right]$ with $b \approx 1.97$ and $r^{*,1} \approx 0.48$ fm, where the value of $r^{*,1}$ sets the scale for the crossing region in Fig. 1. In case of two bound states, we find $b \approx 1.97$ as before and $r^{*,2} \approx 0.20$ fm. The exponents are in very good agreement with our expectations, while $r^{*,1}$ and $r^{*,2}$ are in qualitatively good agreement with our findings in Fig. 2, especially considering the short-distance scale in the deuteron wave function. The resulting hard core pushes the deuteron wave function out from the center, which we see in the second panel of Fig. 2. When enforcing two bound states, instead, the OPE is probed also at smaller r, so that two bound states can be accommodated. In this case, $r^{*,2}$ is smaller than $r^{*,1}$, which leads to smaller values of the LECs (a smaller hard core) at a certain R_0^{-1}. Our results for large R_0^{-1} and n deuteron bound states show that there exists an effective cutoff $r^{*,n}$ in coordinate space. It would further be interesting to investigate how this behavior translates to nonlocal interactions.

We emphasize that all LECs for all numbers of bound states are fit to reproduce NN phase shifts and that this represents an ambiguity when fitting nuclear forces to the phase shifts. Because experimentally there exists only one bound state in the

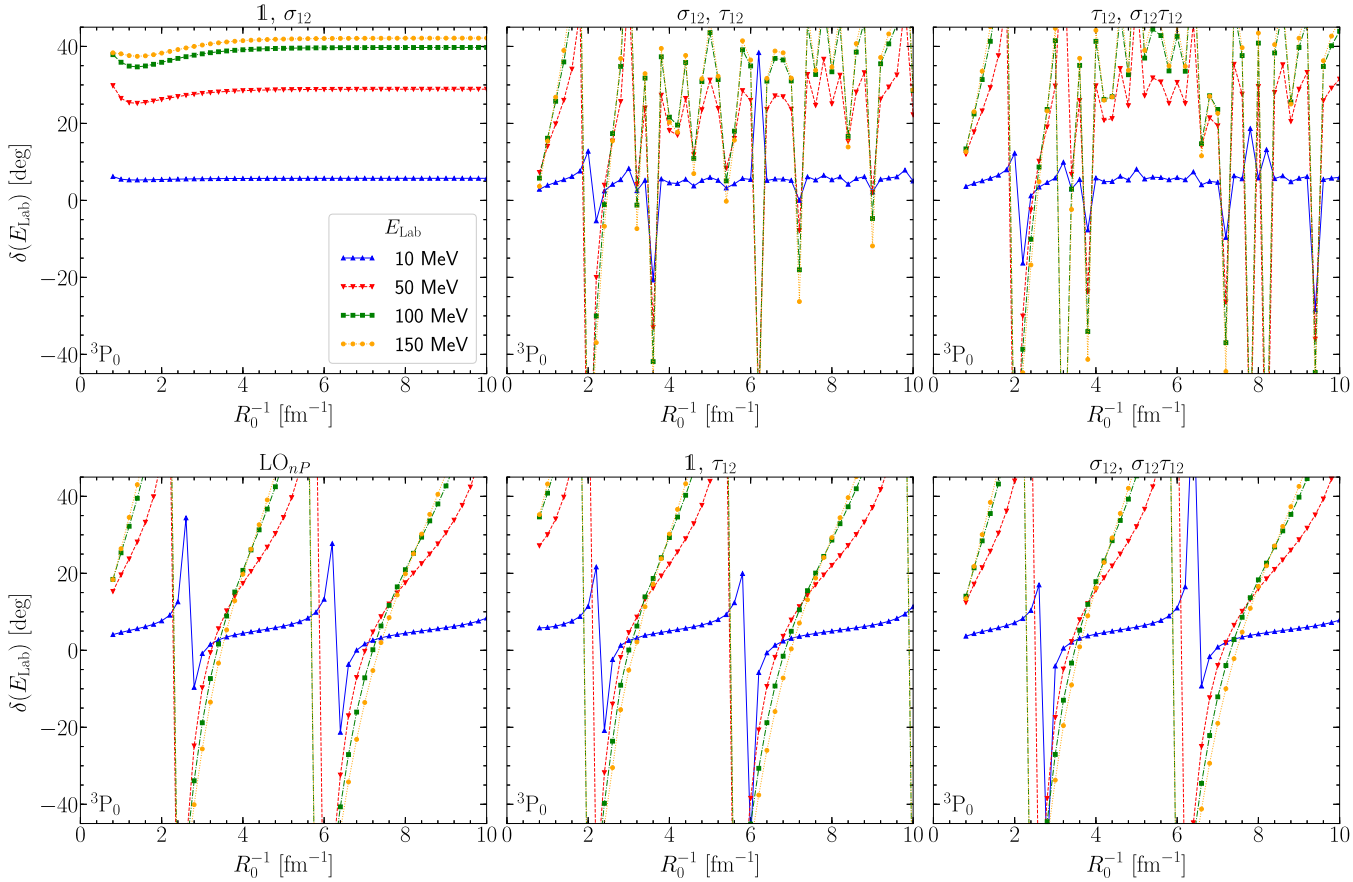

FIG. 3. Phase shifts in the $^3P_0$ partial wave at laboratory energies $E_{\rm lab} = 10$, 50, 100, and 150 MeV vs the inverse cutoff R_0^{-1} for different LO operator structures and $n_1 = n_2 = n = 2$. The first panel shows the phase shifts for the operator pair $\mathbb{1}$, σ_{12}, where the spin-isospin LEC C_{11} is equal to C_{10}. The second and third panels show the operator combinations σ_{12}, τ_{12} and τ_{12}, $\sigma_{12}\tau_{12}$, where $C_{11} \sim -C_{10}$ (see Table I). In the lower panels, we show the interaction LO$_{nP}$, where $C_{11} = 0$ and which is closest to an interaction that respects Fierz rearrangement freedom, as well as the operator combinations $\mathbb{1}$, τ_{12} and σ_{12}, $\sigma_{12}\tau_{12}$, where $C_{11} \sim C_{01}$ with $C_{01} \to 0$ (see Fig. 1). In the lower panels, we find a behavior similar to that in Ref. [8].

deuteron channel, in the following we require our interactions to be on the one-bound-state branch.

III. RESULTS FOR PHASE SHIFTS

Next, we investigate the phase-shift behavior as function of the cutoff scale. We focus on the regulator with $n_1 = n_2 = n = 2$, because this allows us to investigate the interaction also at large values for the inverse cutoff. For this set, we construct potentials for all five linearly independent operator pairs from Eq. (3) and the LO$_{nP}$ potential. Because all interactions are fit to the two S-wave channels, we obtain the same LECs C_{10} and C_{01}, but the LECs C_{00} and C_{11} depend on the operator choice; see Eq. (6) and Ref. [23]. The values of C_{00} and C_{11} for all operator pairs are listed in Table I, where we show both the functional dependence on C_{10} and C_{01} for each LEC, as well as the limit for $R_0 \to 0$ (see Fig. 1). The LECs C_{00} and C_{11} of the LO $_{nP}$ interaction are exactly zero by construction.

In Fig. 3, we show the $^3P_0$ phase shifts at laboratory energies $E_{\rm lab} = 10$, 50, 100, and 150 MeV as function of the inverse cutoff for each of the operator pairs and for the LO$_{nP}$ interaction. In general, when increasing the momentum-space cutoff, i.e., taking the coordinate-space cutoff $R_0 \to 0$, the short-range regulator $f_s(r, R_0)$ becomes narrower. The long-range regulator $f_l(r, R_0)$, on the other hand, which is used in the OPE to suppress the singularity at $r = 0$ while preserving long-range physics, allows more contributions at small distances. In partial waves, where the OPE tensor part is

TABLE I. Leading-order spin-isospin LECs C_{ST} in the $S = 1$, $T = 1$ and $S = 0$, $T = 0$ channels as functions of the coupling constants C_{10} and C_{01} for different operator choices. For LO$_{nP}$, $C_{11} = C_{00} = 0$ by definition. The second columns indicate the limit for $R_0 \to 0$.

Operators	C_{11}		C_{00}	
	Exact	$R_0 \to 0$	Exact	$R_0 \to 0$
$\mathbb{1}$, σ_{12}	C_{10}	$+\infty$	C_{01}	0^-
$\mathbb{1}$, τ_{12}	C_{01}	0^-	C_{10}	$+\infty$
σ_{12}, τ_{12}	$-\frac{1}{2}(C_{10} + C_{01})$	$-\infty$	$\frac{3}{2}(C_{10} + C_{01})$	$+\infty$
σ_{12}, $\sigma_{12}\tau_{12}$	$-\frac{1}{3}C_{01}$	0^+	$-3C_{10}$	$-\infty$
τ_{12}, $\sigma_{12}\tau_{12}$	$-\frac{1}{3}C_{10}$	$-\infty$	$-3C_{01}$	0^+

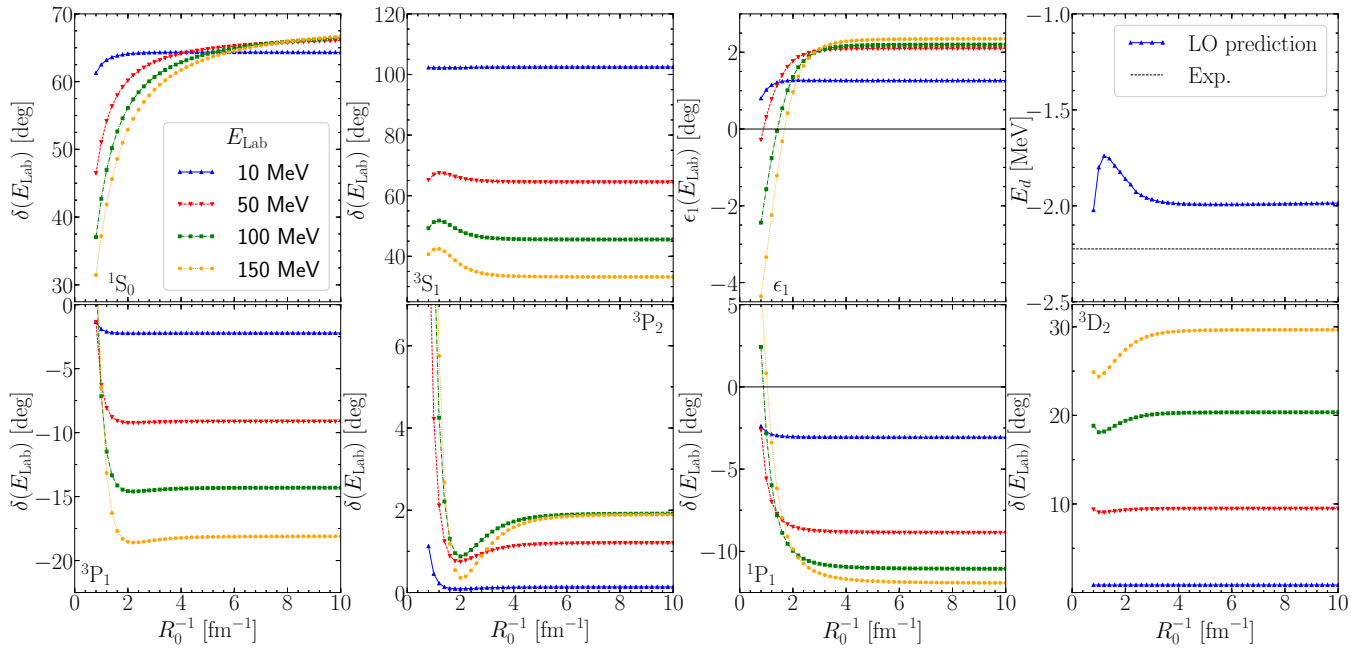

FIG. 4. Phase shifts in the $^1S_0$, $^3S_1$, ϵ_1, $^3D_2$, $^1P_1$, $^3P_1$, and $^3P_2$ partial waves for laboratory energies $E_{\rm lab} = 10, 50, 100$, and 150 MeV as well as the deuteron ground-state energy E_d (upper right panel) as functions of the inverse cutoff R_0^{-1} for the operators $(\mathbb{1}, \sigma_{12})$ and $n_1 = n_2 = n = 2$.

attractive and no counterterms are present, e.g., $^3P_0$, spurious bound states appear. The signature of this effect is a limit-cycle-like behavior of the phase shift [8].

In the first row, we show the operator pairs $(\mathbb{1}, \sigma_{12})$, (σ_{12}, τ_{12}), and $(\tau_{12}, \sigma_{12}\tau_{12})$, for which $C_{11} \sim C_{10}$. For the pair $(\mathbb{1}, \sigma_{12})$, the LEC is repulsive $C_{11} > 0$ and thus acts to compensate the attractive tensor contribution from the OPE interaction. In this case, we find the results stabilize on plateaus when the cutoff is increased. This is the only operator pair for which we observe that the phase shifts become independent of R_0^{-1} for large R_0^{-1}. For the other two operator pairs, the corresponding LEC is attractive, $C_{11} < 0$, which adds to the OPE attraction and leads to the appearance of spurious bound states in the $^3P_0$ wave. This causes a highly oscillatory behavior of the phase shifts.

In the second row, we show the $\mathrm{LO}_{\mathrm{n}P}$, $(\mathbb{1}, \tau_{12})$, and $(\sigma_{12}, \sigma_{12}\tau_{12})$ interactions for which $C_{11} \to 0$. For the $\mathrm{LO}_{\mathrm{n}P}$ interaction, the P waves only receive contributions from OPE, and thus this interaction has the closest resemblance to nonlocal chiral EFT interactions (i.e., to the case studied in Ref. [8]). The other two interactions lead to short-range contributions in the $^3P_0$ wave, but these are small, and the overall phase shifts are very similar to the $\mathrm{LO}_{\mathrm{n}P}$ interaction. Phase-shift jumps in Fig. 3 correspond to cutoff values where new bound states enter in the $^3P_0$ wave. For the interactions in the lower panels, we find a limit-cycle-like behavior similar to the nonlocal potentials of Ref. [8] without counterterms.

For the interaction with operators $(\mathbb{1}, \sigma_{12})$, which leads to plateaus, we show the phase shifts in the $^1S_0$, $^3S_1$, $^3P_1$, $^3P_2$, $^1P_1$, and $^3D_2$ partial waves as well as the mixing angle ϵ_1 and the deuteron ground-state energy in Fig. 4, and find plateaus in all cases for $R_0^{-1} \gtrsim 4$ fm^{-1}, similar to Ref. [8] when counterterms were included there. At higher laboratory energies, the plateau is reached for higher values of R_0^{-1}. The plateau values for the phase shifts are very similar to the results found by NTvK [8], except in the attractive-tensor P and D waves, without adding any new counterterms, in contrast to NTvK. For the deuteron, we find a ground-state energy of $E_d \to -1.99$ MeV for $R_0^{-1} \to \infty$, which is close to experiment although the deuteron was not included in the fit.

In Fig. 5, we show the phase shifts as function of R_0^{-1} in three partial waves for different laboratory energies and different regulator choices. We find that the phase shifts converge to the same values, and that the plateaus are independent of the exponents in the regulator functions. Note that for the sets $\{n_1, n_2, n\} = \{2, 2, 4\}$ and $\{4, 1, 4\}$ we do not obtain numerical results for $R_0^{-1} > 4.4$ fm^{-1} as discussed for Fig. 1.

The phase shift plateaus do not necessarily have to be close to the physical phase shift values. In Fig. 6, we compare the phase shifts as functions of the laboratory energy in several partial waves for two cutoff scales ($R_0^{-1} = 1.0$ fm^{-1} and $R_0^{-1} = 10$ fm^{-1}) with the PWA values. The large-cutoff interaction that lies on the phase-shift plateaus describes the energy dependence of the phase shifts reasonably well and in some cases much better than the result for a typical low cutoff. The only exception is the $^1S_0$ partial wave, because at LO the effective range cannot be correctly described. It is not clear if an improvement can be found at NLO due to causality bounds [24], and it will be interesting to investigate the order-by-order behavior at large R_0^{-1}.

IV. DISCUSSION

Because of the attractive singular OPE, results are very cutoff dependent in WPC without the promotion of additional counterterms. In this paper, we have explained the fact that

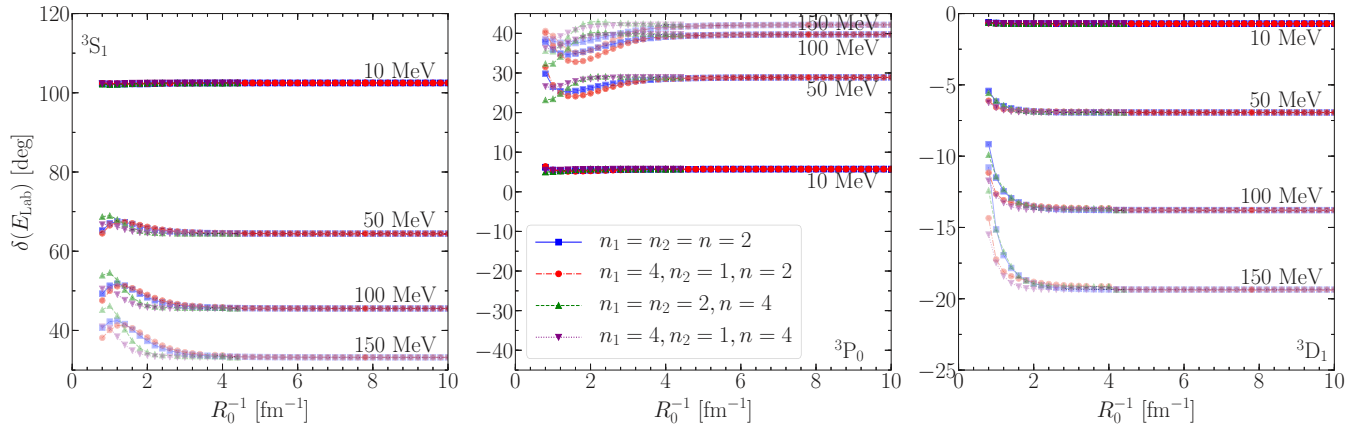

FIG. 5. Phase shifts in the $^3S_1$, $^3P_0$, and $^3D_1$ partial waves for different laboratory energies and for different regulator functions, as functions of the inverse cutoff R_0^{-1} for the operators $(\mathbb{1}, \sigma_{12})$.

local regulators connect the LO counterterms with all higher partial waves. For a certain class of local regulators, these regulator artifacts can compensate the attractive tensor contributions from OPE and we find cutoff-independent results. However, we state explicitly that these results do not imply that WPC is renormalizable.

We investigated an interesting case for local interactions, which may be beneficial from a practical point of view as

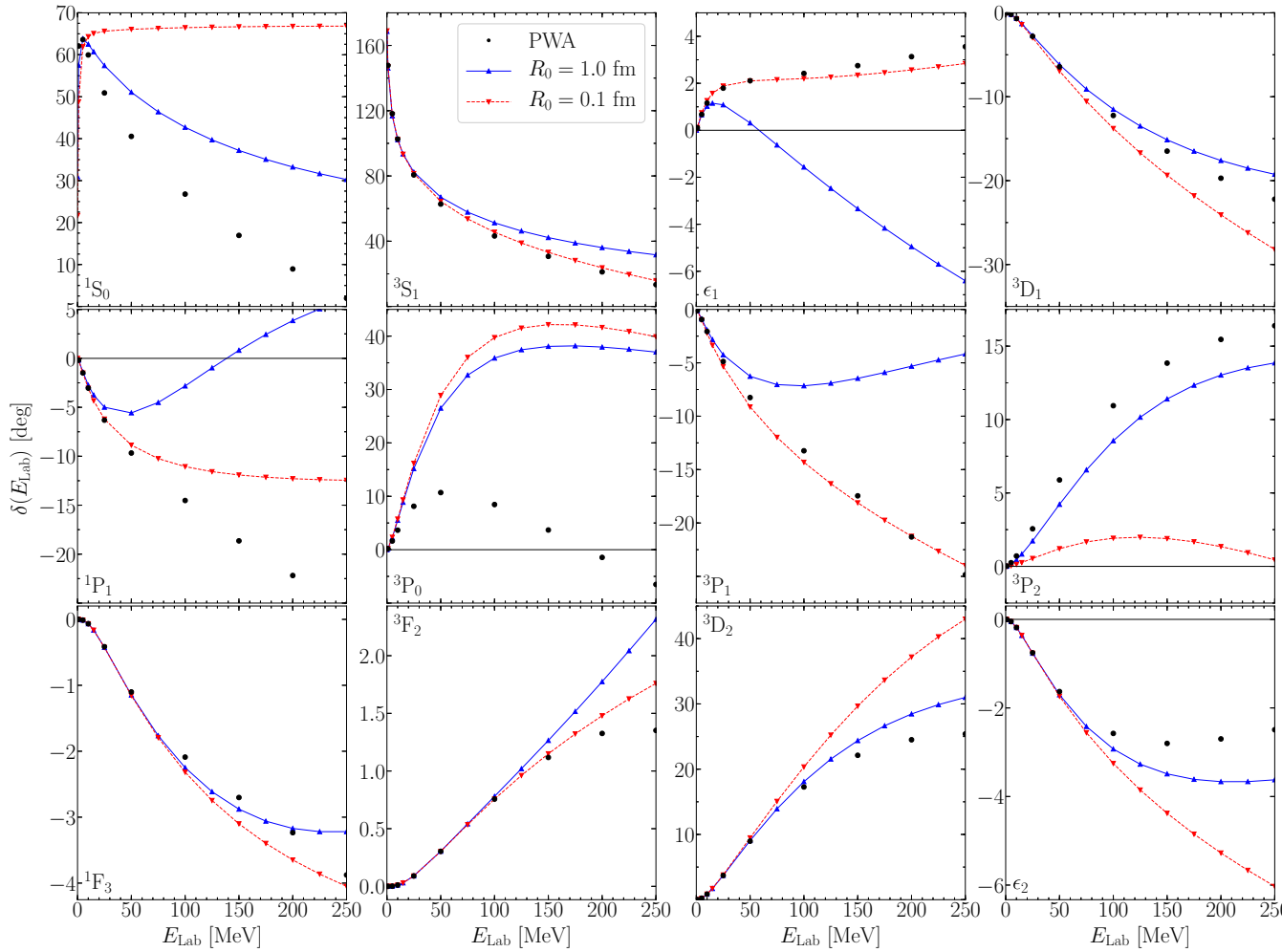

FIG. 6. Phase shifts in the $^1S_0$, $^3S_1$, ϵ_1, $^3D_1$, $^1P_1$, $^3P_{0,1,2}$, $^1F_3$, $^3F_2$, ϵ_2, and $^3D_2$ channels as function of the laboratory energy for the inverse cutoffs $R_0^{-1} = 1\,\text{fm}^{-1}$ and $R_0^{-1} = 10\,\text{fm}^{-1}$ for $n_1 = n_2 = n = 2$ in comparison to the PWA phase shifts.

local interactions with larger R_0^{-1} can easily be explored with quantum Monte Carlo methods and may allow to reduce regulator artifacts in many-body systems. In Ref. [25], it was found that lowering the $3N$ cutoff R_{3N} in pure neutron matter while keeping a constant NN cutoff R_0 leads to collapses of the many-body system. The best result was found when $R_{3N} = R_0$. If it is possible to construct chiral interactions with smaller NN cutoff and no spurious bound states, as we have shown here, one can lower the $3N$ cutoff while at the same time avoiding such collapses. This will help to reduce $3N$ regulator artifacts, which have been found to be sizable; see Refs. [22,26]. This may therefore allow to significantly reduce uncertainties in many-body calculations with local chiral interactions. The results of such calculations will be reported in a future paper.

Conceptually, our results are very different from the results of NTvK. While NTvK restore renormalizability of chiral interactions at LO by adding additional counterterms in channels with attractive tensor interactions and then obtain cutoff-independent results, we have seen that the regulator artifacts for local chiral interactions with the operator combination $(\mathbb{1},\ \sigma_{12})$ add additional repulsion to the same partial waves, which in turn leads to similar plateaus; see Fig. 3. However, the appearance of plateaus does not mean that our interactions are renormalizable.

Our findings are only possible for certain local regulators that are smooth functions. Furthermore, the appearance of plateaus is only possible because we require the interactions to remain on the branch for a single bound state in the deuteron channel. As we have explored before, in this case the width of the short-range regulator function decreases with R_0^{-1} but this is compensated by increasing values of the LECs. This results in a nonvanishing hard core which compensates the attraction from OPE in such a way that only one bound state can be accommodated.

The core is strong enough to counter the attraction in the ${}^3S_1$-${}^3D_1$ channel (where it is strongest), and it is only natural that it is sufficiently strong to counter the attraction in higher partial waves, where we find no additional spurious bound states. This is another difference from the results of NTvK, where the introduction of additional counterterms does not eliminate the appearance of spurious bound states. If we instead allow for more bound states to appear in the ${}^3S_1$ channel, the values of the LECs decrease and the core is reduced in magnitude. Then, we also find a limit-cycle cutoff dependence behavior and additional counterterms need to be added in the attractive tensor channels, as NTvK found.

We remark, however, that if we would allow more bound states to enter, this would mean that the LECs $C_{ST}(R_0)$ have to jump from one bound-state branch to another bound-state branch. To our knowledge, in this case there is no clear prescription at which cutoff values these jumps have to occur, which introduces an additional ambiguity. Enforcing one bound state, on the other hand, is a reasonable and practical prescription for the construction of potentials that introduces no new ambiguity.

While the connection of the S-wave contact interactions with higher partial waves is purely a regulator artifact, such a connection can have a qualitative physical motivation. The LO counterterms in WPC absorb, among others, the effects of heavier mesons like the ρ or ω meson, which are integrated out in chiral EFT [27]. Such heavier mesons are responsible for the short-range NN repulsion and compensate the singular attraction of the OPE interaction; see also Ref. [14]. The exchange interactions for these mesons are local in the static limit and enter all partial waves, similarly to pion exchanges. Local regulators establish a similar connection of all partial waves.

For example, the central short-range repulsion in one-boson-exchange potentials originates from ω-meson exchange [28]. The exchange potential of a very heavy ω-like vector meson would be given by

$$V_\omega(m_\omega, r) \xrightarrow{m_\omega \gg m_N} \frac{e^{-M_\omega r}}{r}\left\{\left(\mathbb{1}+\frac{1}{3}\sigma_{12}\right) -\frac{1}{6}\left[1+\frac{3}{M_\omega r}+\frac{3}{(M_\omega r)^2}\right]S_{12}(\mathbf{r})\right\} \tag{10}$$

with the mass of the meson m_ω and the nucleon mass m_N; see, e.g., Eq. (F.8) in Ref. [28]. In the case of the local LO potential with the operator structure $(\mathbb{1}, \sigma_{12})$, we find that the operator LECs for larger cutoffs approach $C_{\mathbb{1}} = 3C_\sigma$, because $C_{01} = C_{\mathbb{1}} - 3C_\sigma \to 0$. Thus, a corresponding meson would need to have the leading operator structure $\sim \mathbb{1} + 1/3\sigma_{12}$, which is exactly the central part of an ω-like vector meson. We highlight this in the left panels of Fig. 2, where, in addition to the results for the central chiral interactions, we also show the result for the ω-meson exchange. We find a behavior similar to the chiral interactions for larger cutoffs.

V. SUMMARY

In this paper, we have investigated the behavior of local chiral interactions in WPC when the coordinate-space cutoff is lowered. We have constructed LO interactions for cutoffs ranging from $R_0^{-1} = 0.8$ to $10.0\ \mathrm{fm}^{-1}$ for different choices of the regulator function and for different pairs of the LO operators of $\{\mathbb{1}, \sigma_{12}, \tau_{12}, \sigma_{12}\tau_{12}\}$. Our interactions were fit to reproduce the S-wave phase shifts from the Nijmegen PWA. We additionally required only one bound state in the deuteron channel but did not use the deuteron binding energy to constrain our fits.

Our results show that, for the operator combination $(\mathbb{1}, \sigma_{12})$, phase shifts in all partial waves as well as the deuteron ground-state energy exhibit a plateau when increasing the inverse cutoff R_0^{-1}, leading to cutoff-independent results. This can be explained because in the fit the attractive tensor contribution from OPE in the deuteron channel is compensated by the short-range contact interactions to guarantee only one bound state. Local regulators mix contributions from all operators into all partial waves, i.e., LO operators that nominally only describe S-wave physics contribute to all channels once a local regulator is used. For the operator choice $(\mathbb{1}, \sigma_{12})$, the LEC C_{10} in the ${}^3S_1$ channel is mixed into all attractive tensor channels with the same sign, providing sufficient repulsion in these channels.

Thus, using the artifacts of local regulators to our advantage allowed us to construct interactions that enable a cutoff-independent description of phase shifts. Comparing the phase-shift predictions for these hard interactions with phase shifts from the PWA, we found very good agreement at LO.

We state again that these results do not imply that WPC is renormalizable. However, our findings may prove useful from a practical point of view, as they may allow to reduce regulator artifacts in many-body calculations. In the future, we will investigate these hard potentials in quantum Monte Carlo calculations of nuclear systems to investigate if this behavior persists.

ACKNOWLEDGMENTS

We thank R. Furnstahl, A. Gezerlis, D. B. Kaplan, S. König, J. Lynn, D. Philips, U. van Kolck, and C. J. Yang for useful discussions. This work was supported in part by the National Science Foundation Grant No. PHY-1430152 (JINA Center for the Evolution of the Elements), the European Research Council Grant No. 307986 STRONGINT, the Deutsche Forschungsgemeinschaft Grant No. SFB 1245, and the U.S. Department of Energy Grant No. DE-FG02-00ER41132. Computational resources have been provided by the Jülich Supercomputing Center and the Lichtenberg high-performance computer of TU Darmstadt.

[1] E. Epelbaum, H.-W. Hammer, and U.-G. Meißner, Rev. Mod. Phys. **81**, 1773 (2009).
[2] R. Machleidt and D. R. Entem, Phys. Rep. **503**, 1 (2011).
[3] S. Weinberg, Physica A **96**, 327 (1979).
[4] S. Weinberg, Phys. Lett. B **251**, 288 (1990).
[5] S. Weinberg, Nucl. Phys. B **363**, 3 (1991).
[6] S. Weinberg, Phys. Lett. B **295**, 114 (1992).
[7] S. R. Beane, P. F. Bedaque, L. Childress, A. Kryjevski, J. McGuire, and U. van Kolck, Phys. Rev. A **64**, 042103 (2001).
[8] A. Nogga, R. G. E. Timmermans, and U. van Kolck, Phys. Rev. C **72**, 054006 (2005).
[9] D. B. Kaplan, M. J. Savage, and M. B. Wise, Phys. Lett. B **424**, 390 (1998).
[10] D. B. Kaplan, M. J. Savage, and M. B. Wise, Nucl. Phys. B **534**, 329 (1998).
[11] V. G. J. Stoks, R. A. M. Klomp, M. C. M. Rentmeester, and J. J. de Swart, Phys. Rev. C **48**, 792 (1993).
[12] S. Fleming, T. Mehen, and I. W. Stewart, Nucl. Phys. A **677**, 313 (2000).
[13] S. R. Beane, P. F. Bedaque, M. J. Savage, and U. van Kolck, Nucl. Phys. A **700**, 377 (2002).
[14] S. R. Beane, D. B. Kaplan, and A. Vuorinen, Phys. Rev. C **80**, 011001 (2009).
[15] M. Pavon Valderrama and E. Ruiz Arriola, Phys. Rev. C **74**, 054001 (2006).
[16] M. Pavon Valderrama and E. Ruiz Arriola, Phys. Rev. C **74**, 064004 (2006).
[17] M. C. Birse, Phys. Rev. C **74**, 014003 (2006).
[18] E. Epelbaum and U.-G. Meißner, Few-Body Syst. **54**, 2175 (2013).
[19] A. Gezerlis, I. Tews, E. Epelbaum, S. Gandolfi, K. Hebeler, A. Nogga, and A. Schwenk, Phys. Rev. Lett. **111**, 032501 (2013).
[20] A. Gezerlis, I. Tews, E. Epelbaum, M. Freunek, S. Gandolfi, K. Hebeler, A. Nogga, and A. Schwenk, Phys. Rev. C **90**, 054323 (2014).
[21] J. E. Lynn, I. Tews, J. Carlson, S. Gandolfi, A. Gezerlis, K. E. Schmidt, and A. Schwenk, Phys. Rev. Lett. **116**, 062501 (2016).
[22] A. Dyhdalo, R. J. Furnstahl, K. Hebeler, and I. Tews, Phys. Rev. C **94**, 034001 (2016).
[23] L. Huth, I. Tews, J. E. Lynn, and A. Schwenk, Phys. Rev. C **96**, 054003 (2017).
[24] D. R. Phillips and T. D. Cohen, Phys. Lett. B **390**, 7 (1997).
[25] I. Tews, S. Gandolfi, A. Gezerlis, and A. Schwenk, Phys. Rev. C **93**, 024305 (2016).
[26] I. Tews, J. Carlson, S. Gandolfi, and S. Reddy, Astrophys. J. **860**, 149 (2018).
[27] E. Epelbaum, U.-F. Meißner, W. Glöckle, and C. Elster, Phys. Rev. C **65**, 044001 (2002).
[28] R. Machleidt, K. Holinde, and C. Elster, Phys. Rep. **149**, 1 (1987).